

See discussions, stats, and author profiles for this publication at: <https://www.researchgate.net/publication/5625754>

Formation of Sugar Radicals in RNA Model Systems and Oligomers via Excitation of Guanine Cation Radical

ARTICLE *in* THE JOURNAL OF PHYSICAL CHEMISTRY B · MARCH 2008

Impact Factor: 3.3 · DOI: 10.1021/jp077429y · Source: PubMed

CITATIONS

22

READS

19

5 AUTHORS, INCLUDING:



Anil Kumar

Oakland University

59 PUBLICATIONS 1,152 CITATIONS

SEE PROFILE



Amitava Adhikary

Oakland University

43 PUBLICATIONS 698 CITATIONS

SEE PROFILE



Michael D Sevilla

Oakland University

222 PUBLICATIONS 6,179 CITATIONS

SEE PROFILE

Formation of Sugar Radicals in RNA Model Systems and Oligomers via Excitation of Guanine Cation Radical

Deepti Khanduri, Sean Collins, Anil Kumar, Amitava Adhikary, and Michael D. Sevilla*

Department of Chemistry, Oakland University, Rochester, Michigan 48309

Received: September 14, 2007; In Final Form: November 19, 2007

In previous work, we have shown that photoexcitation of guanine cation radical ($G^{\bullet+}$) in frozen aqueous solutions of DNA and its model compounds at 143 K results in the formation of neutral sugar radicals with substantial yield. In this report, we present electron spin resonance (ESR) and theoretical (DFT) evidence regarding the formation of sugar radicals after photoexcitation of guanine cation radical ($G^{\bullet+}$) in frozen aqueous solutions of one-electron-oxidized RNA model compounds (nucleosides, nucleotides and oligomers) at 143 K. Specific sugar radicals $C5^{\bullet}$, $C3^{\bullet}$ and $C1^{\bullet}$ were identified employing derivatives of Guo deuterated at specific sites in the sugar moiety, namely, $C1'$ –, $C2'$ –, $C3'$ – and $C5'$ –. These results suggest $C2^{\bullet}$ is not formed upon photoexcitation of $G^{\bullet+}$ in one-electron-oxidized Guo and deuterated Guo derivatives. Phosphate substitution at $C5'$ – (i.e., in 5-GMP) hinders formation of $C5^{\bullet}$ via photoexcitation at 143 K but not at 77 K. For the RNA-oligomers studied, we observe on photoexcitation of oligomer- $G^{\bullet+}$ the formation of mainly $C1^{\bullet}$ and an unidentified radical with a ca. 28 G doublet. The hyperfine coupling constants of each of the possible sugar radicals were calculated employing the DFT B3LYP/6-31G* approach for comparison to experiment. This work shows that formation of specific neutral sugar radicals occurs via photoexcitation of guanine cation radical ($G^{\bullet+}$) in RNA systems but not by photoexcitation of its N1 deprotonated species ($G(-H)^{\bullet}$). Thus, our mechanism regarding neutral sugar formation via photoexcitation of base cation radicals in DNA appears to be valid for RNA systems as well.

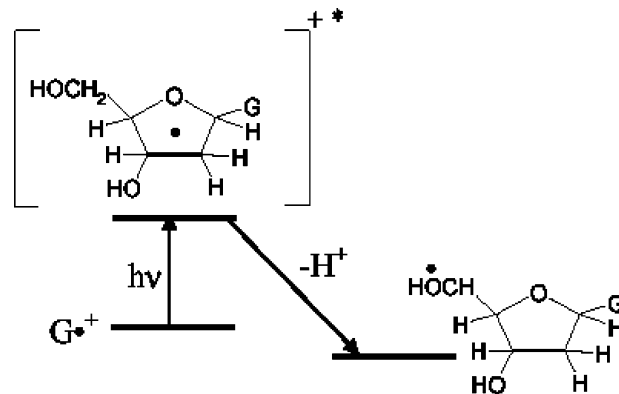
Introduction

Shukla et al.¹ first reported the formation of sugar radicals on photoexcitation of guanine cation radical ($G^{\bullet+}$) in DNA. They proposed that excitation of guanine cation radical ($G^{\bullet+}$) results in delocalization of a significant fraction of the spin and charge onto the sugar moiety to form a transient sugar cation radical ($S^{\bullet+}$) that undergoes rapid deprotonation resulting in a neutral sugar radical. This hypothesized mechanism is illustrated in Scheme 1, showing excited guanine cation radical [$(G^{\bullet+})^*$] leads to formation of $C5^{\bullet}$ in dGuo.²

A number of our recent studies^{2–8} have validated the mechanism shown in Scheme 1. We found that visible photoexcitation of $G^{\bullet+}$ (in dGuo)² and one-electron-oxidized adenine in dAdo³ in aqueous glassy systems lead to formation of sugar radicals $C5^{\bullet}$ and $C3^{\bullet}$ as well as some $C1^{\bullet}$. These experimental observations were also supported by time-dependent density functional theory (TD-DFT) calculations which suggest core excitations (i.e., excitation from the inner shell molecular orbitals) in $G^{\bullet+}$ of dGuo or in one-electron-oxidized adenine of dAdo to the singly occupied molecular orbital (SOMO) are responsible for the delocalization of the spin and charge onto the sugar moiety.^{2,3} Moreover, with the aid of dGuo and dAdo derivatives having selective isotopic substitution in the sugar moiety (e.g., deuteration in dGuo² and ¹³C substitution in dAdo³), we have successfully identified each of the sugar radicals.

Our studies involving DNA-nucleosides, DNA-nucleotides^{2,3} and DNA-oligomers^{4–8} have established that the type of sugar

SCHEME 1: Formation of a Sugar Radical, e.g., $C5^{\bullet}$, via Photoexcited $G^{\bullet+}$



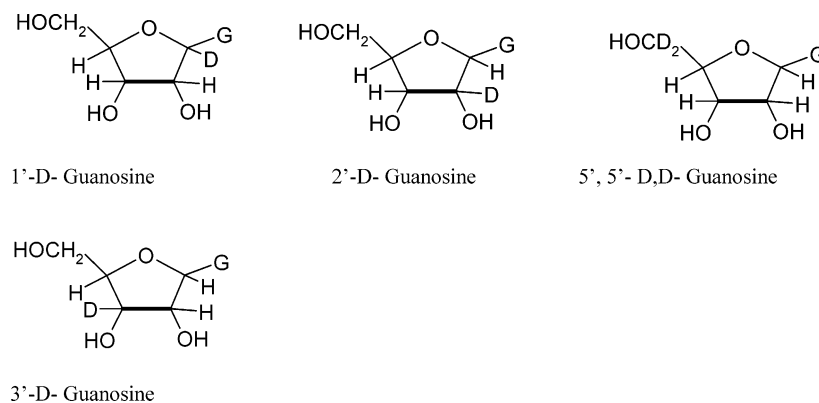
radical (i.e., specific site of deprotonation at the deoxyribose sugar (see Scheme 1) as well as the sugar radical cohort are crucially influenced by

(i) Site of phosphate substitution (either 3'– or 5'–): Phosphate substitution at a 3'– or 5'– site in a nucleoside deactivates the site toward formation of a sugar radical. For example, photoexcitation of $G^{\bullet+}$ leads to the formation of $C5^{\bullet}$, $C3^{\bullet}$ and $C1^{\bullet}$ in dGuo, whereas we found predominant production of $C1^{\bullet}$ (with a small extent of $C3^{\bullet}$ formation) in 5'-dGMP and of $C5^{\bullet}$ and $C1^{\bullet}$ in 3'-dGMP.²

(ii) pH: Conversion of one-electron-oxidized guanine to sugar radicals is effective for its cation radical ($G^{\bullet+}$) in dGuo,^{2,9} dinucleoside phosphates,^{4,6–8} DNA-oligomers^{4,6} and presumably in DNA^{2,7} but far less so for its N1 deprotonated state ($G(-H)^{\bullet}$).^{2,7–11} However, for dAdo and its derivatives, formation of

* Author for correspondence. E-mail: sevilla@oakland.edu. Phone: 001 248 370 2328. Fax: 001 248 370 2321.

SCHEME 2: Isotopically Substituted Compounds Used



sugar radicals via excitation of one-electron-oxidized adenine occurs at all pHs investigated, that is, from pH 5 to 12.^{3,7}

(iii) Wavelength, that is, excitation energy, of the incident light: Wavelengths in the range 310–650 nm of light are found to be effective in the formation of sugar radicals via photoexcitation of $G^{\bullet+}$ in model compounds, that is, in deoxynucleosides, deoxynucleotides and also in short DNA-oligomers such as TGGT.^{2,6,7} On the other hand, sugar radical formation via photoexcitation of $G^{\bullet+}$ in γ -irradiated, hydrated ($\Gamma = 12 \text{ D}_2\text{O}/\text{nucleotide}$) DNA is wavelength dependent.² In the 310–480 nm range, formation of $C1^{\bullet}$ in substantial yields has been observed in double-stranded DNA (dsDNA) via photoexcitation of $G^{\bullet+}$ from 77 to 180 K but little conversion occurs at longer wavelengths.^{2,6}

(iv) Length of the oligomer: For longer DNA-oligomers such as TTGGTTGGTT, there is a relative increase in the formation of $C1^{\bullet}$ compared with shorter DNA-oligomers;⁶ light with wavelengths $> 500 \text{ nm}$ becomes less effective at forming sugar radicals from $G^{\bullet+}$ likely as a result of base-to-base hole transfer as the oligomer length increases.⁶ Such base-to-base hole transfer was predicted by TD-DFT calculations in dinucleoside phosphates.^{4,5,7,8} The extent of photoconversion of $G^{\bullet+}$ to sugar radicals, as well as its initial rate of conversion, decreases with increasing size of the oligonucleotides, although it still remains substantial (50%) even for high molecular weight salmon testes DNA.⁶

In this study, we extend our investigations from DNA to RNA systems including nucleosides, nucleotides and oligonucleotides in order to answer the following questions:

(1) What are the identities of the sugar radicals formed in RNA-nucleosides via photoexcitation of one-electron-oxidized guanine? Because of the variety of sugar radical conformations defined by the pseudorotation cycle,¹² we expect that identification of sugar radicals in RNA systems based on their hyperfine splitting will be difficult, since the RNA-sugar radicals, like their corresponding DNA-sugar radicals, are able to adopt numerous conformations.¹³ Therefore, we employ selective isotopic substitution of deuterium (at $C1'$, $C2'$, $C3'$ and $C5'$) in the sugar moiety to positively identify radical species. Moreover, using DFT calculations employing the B3LYP/6-31G* method, we have calculated expected proton hyperfine couplings of these radicals and have compared these results with the corresponding experimentally obtained values.

(2) In one-electron-oxidized RNA systems, do both the guanine cation radical ($G^{\bullet+}$) and its N1 deprotonated species ($G(-H)^{\bullet}$) produce sugar radicals? Or, does only $G^{\bullet+}$ lead to form sugar radicals as observed in the case of DNA systems?

(3) Does the site of phosphate substitution affect the likelihood

of sugar radical formation via photoexcitation at that site in RNA systems as found for DNA systems?

(4) What are the identities of sugar radicals formed in RNA-oligomers via photoexcitation of one-electron-oxidized guanine?

This investigation seeks to answer each of these questions. We note that OH-radical-induced strand breakage in RNA has been studied extensively using poly(U) as a model system.^{11h,14} The high G value for strand breakage in poly(U)¹⁵ has been explained using two mechanisms: (i) direct H-atom abstraction by the OH-radical from the $C2'$ - site in the sugar moiety and (ii) formation of $C2^{\bullet}$ via $C2'$ -H abstraction by the initially produced base radical.^{11h,14} For this reason and also for the fact that the $C2'$ -H bond is predicted to be the weakest in RNA,¹⁶ we expected dominant formation of $C2^{\bullet}$ in RNA-oligomers after photoexcitation of RNA-oligomers containing one-electron-oxidized guanine. It was therefore surprising that in this study we find that the sugar radical cohort formed via photoexcitation of one-electron-oxidized RNA-oligomers contains significant amounts of $C1^{\bullet}$ and a second unidentified radical species. This observation is in agreement with our previous work showing formation of $C1^{\bullet}$ in DNA-oligomers and in high molecular weight DNA.^{1,2,6}

Materials and Methods

RNA Model Compounds. Guanosine (Guo), guanosine 5'-monophosphate (5'-GMP) and lithium chloride (99% anhydrous, SigmaUltra) were obtained from Sigma Chemical Company (St Louis, MO). Potassium persulfate (crystal) was purchased from Mallinckrodt, Inc. (Paris, KY). We have purchased 1'-D-guanosine (1'-D-Guo), 2'-D-guanosine (2'-D-Guo), 3'-D-guanosine (3'-D-Guo) and 5',5'-D,D-guanosine (5',5'-D,D-Guo) (see Scheme 2) from Omicron Biochemicals, Inc. (South Bend, IN). All of these deuterated derivatives were synthesized by Omicron from D-ribose so that the stereospecificity of the deuteration was maintained. All chemicals were used without further purification.

RNA-Oligomers. The RNA-oligomers UGGGU, UAGAU, UUGGUU, UUCGAA and UCGCU used in this study were all obtained from IDT-Synthegen with standard desalting (Corville, IA). All of these RNA-oligomers were also used without further purification.

Glassy Sample Preparation. For preparation of glassy samples of nucleosides, nucleotides and deuterated derivatives, ca. 3 mg of the compound was dissolved in 1 mL of 7.5 M LiCl in D_2O in the presence of 5 mg of $\text{K}_2\text{S}_2\text{O}_8$, as per our earlier works with DNA-nucleosides and -nucleotides.^{1-3,9} For preparation of glassy samples of RNA-oligomers, about 1.5 mg of each of the RNA-oligomers was dissolved in 0.35 mL of 7.5

M LiCl in D₂O in the presence of 2.5 mg of K₂S₂O₈, as per our earlier works with DNA-oligomers.^{4,6} Then, these solutions were thoroughly bubbled with nitrogen. Using these solutions, the transparent glassy samples were prepared by drawing the solution into 4 mm Suprasil quartz tubes (cat. no. 734-PQ-8, WILMAD Glass Co., Inc., Buena, NJ) followed by cooling to 77 K. All samples are stored at 77 K.

“pH” Adjustments. Following our earlier work,^{2,3,9} if required, the pH was adjusted by adding microliter amounts of concentrated HCl under ice-cooled conditions. pH papers were used to check the pH values, and owing to the high ionic strength of the LiCl solution (7.5 M), the pH values reported in this work are approximate ones. We note here that we have determined the “pH” for D₂O solutions (pD).^{2,3,9}

γ -Irradiation. As per our earlier works,^{1–4,6,9} all glassy samples of nucleosides and their deuterated derivatives, of nucleotides, and of RNA-oligomers were γ -irradiated under liquid nitrogen using a model 109-GR9 irradiator, containing a shielded ⁶⁰Co source. Glassy samples of nucleosides and their deuterated derivatives and of nucleotides were γ -irradiated (⁶⁰Co) with an absorbed dose of 2.5 kGy at 77 K. For glassy samples of RNA-oligomers, the absorbed dose was 5 kGy at 77 K.

Annealing of Samples. Following our previous works,^{1–4,6,9} a variable temperature assembly has been applied to carry out annealing of the samples. We have used a copper-constantan thermocouple in direct contact with the sample to monitor the temperatures during annealing. As per our works in 2'-deoxynucleosides/tides^{1–3,9} and DNA-oligomers,^{4,6} annealing of the glassy samples (7.5 M LiCl/D₂O) stored at 77 K to 150–155 K for 10–20 min results in the loss of Cl₂^{•−} with the concomitant formation of G^{•+}. We also note that, similar to our works in 2'-deoxynucleosides/tides^{1–3} and DNA-oligomers,^{4,6} sugar radical formation was not observed by direct attack of Cl₂^{•−} on the sugar moiety in these RNA-nucleosides/tides and RNA-oligomers during annealing.

Photoexcitation of Samples. Photoexcitation of these glassy samples of nucleosides and 5'-GMP, of nucleosides with selective isotopic substitution and of RNA-oligomers containing one-electron-oxidized guanine was carried out using a photo-flood lamp (250 W) with a water filter (for IR components) and a 310 nm cut off filter for UV components. No filter in the visible was employed. We note that, under our experimental conditions, only a small amount (ca. 60 mW) of the total lamp intensity is active at the sample.³

Electron Spin Resonance. The glassy samples after γ -irradiation at 77 K, annealing to 155 K and photoexcitation at 143 K were immediately immersed in liquid nitrogen. As per our earlier works,^{1–4,9} an electron spin resonance (ESR) spectrum was then recorded at 77 K and 40 dB (20 μ W) and Fremy's salt (with $g = 2.0056$, $A_N = 13.09$ G) was used for field calibration (shown as triangular reference marks in all figures with ESR spectra).

The ESR spectra of the samples were recorded using a Varian Century Series ESR spectrometer operating at 9.2 GHz with an E-4531 dual cavity, a 9 in. magnet and a 200 mW klystron.

As done in our earlier works with the glassy samples of 2'-deoxynucleosides/tides^{2,3} and of the DNA-oligomers,^{6,9} subtraction of a small singlet “spike” from irradiated quartz at $g = 2.0006$ was removed from the recorded spectra before the analyses.

Analysis of ESR Spectra. From doubly integrated areas of benchmark spectra, the fraction that a particular radical contributes to an overall spectrum is estimated. The doubly

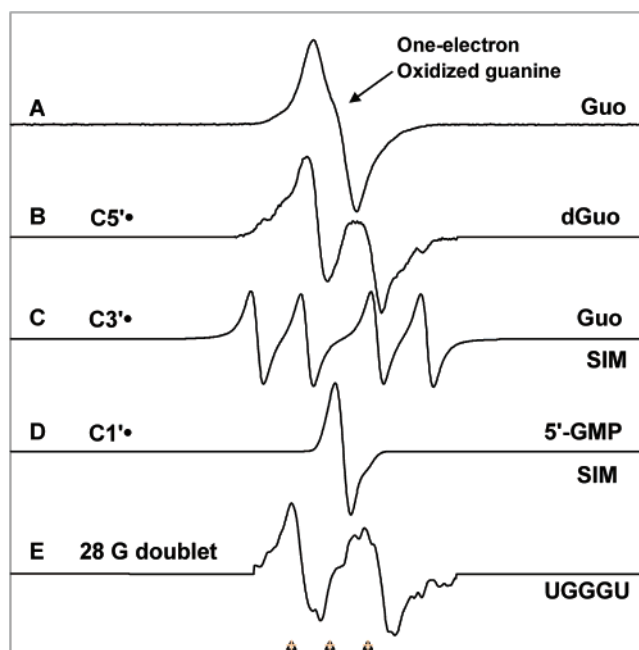


Figure 1. (A) One-electron-oxidized guanine from Guo at native pH (ca. 5) of 7.5 M LiCl glass. (B) C5[•], produced by photoexcitation of one-electron-oxidized guanine in 3'-dGMP.² (C) Simulated spectrum for C3[•] obtained in Guo using two β -hydrogen hyperfine couplings, 41 and 17 G, with a 4.5 G line width and $g_{\text{iso}} = 2.0028$ (see text and Table 1). (D) Benchmark spectrum of C1[•] represented employing suitable anisotropic simulation. (E) A doublet ca. 28 G isolated from UGGGU (see text). The three triangular calibration markers shown in this figure and in all the other figures in this work represent positions of Fremy's salt resonances (the central marker is at $g = 2.0056$, and each of three markers is separated from one another by 13.09 G).

integrated areas are directly proportional to the number of spins of each radical species (moles of each radical). Least-squares fittings of benchmark spectra (Figure 1) have been employed to determine the fractional composition of radicals in experimental spectra using programs (ESRPLAY, ESRADSUB) written in our laboratory.

The benchmark spectra used for analyses of the ESR spectra presented in this work are shown in Figure 1. The benchmark spectrum for one-electron-oxidized guanine is derived via one-electron oxidation of guanosine by Cl₂^{•−} (Figure 1A). The benchmark spectrum for C5[•] (Figure 1B) has already been derived from dGuo.² The benchmark spectrum for C3[•] in Guo samples shown in Figure 1C is obtained with the aid of isotropic simulation using experimental couplings of 41 G (1 β H) and 17 G (1 β H). The β -proton couplings at C2'– and C4'– protons were assigned from selective deuterium substitution in the sugar moiety (vide infra). We have isolated the singlet spectrum of C1[•] in 5'-GMP via subtraction of the spectrum of one-electron-oxidized guanine from the spectrum obtained after 25 min of photoexcitation in 5'-GMP samples (see Figure 5C). In Figure 1D, we mimicked this singlet spectrum for C1[•] employing anisotropic simulation. We have also found a doublet with a hyperfine coupling of ca. 28 G obtained from UGGGU and have employed it as a benchmark spectrum for analyzing the spectra of RNA-oligomers.

The radicals described in this work are presented in Scheme 3. The hyperfine coupling constant (HFCC) values of the sugar radicals and their apparent g -values are mentioned in Table 1.

DFT Calculations. Geometries of guanosine cation radical (Guo^{•+}) in C3'-endo-C2'-exo and C2'-endo-C3'-exo conformations were optimized using Becke's three-parameter exchange functionals (B3)¹⁷ with Lee, Yang and Parr's correlational

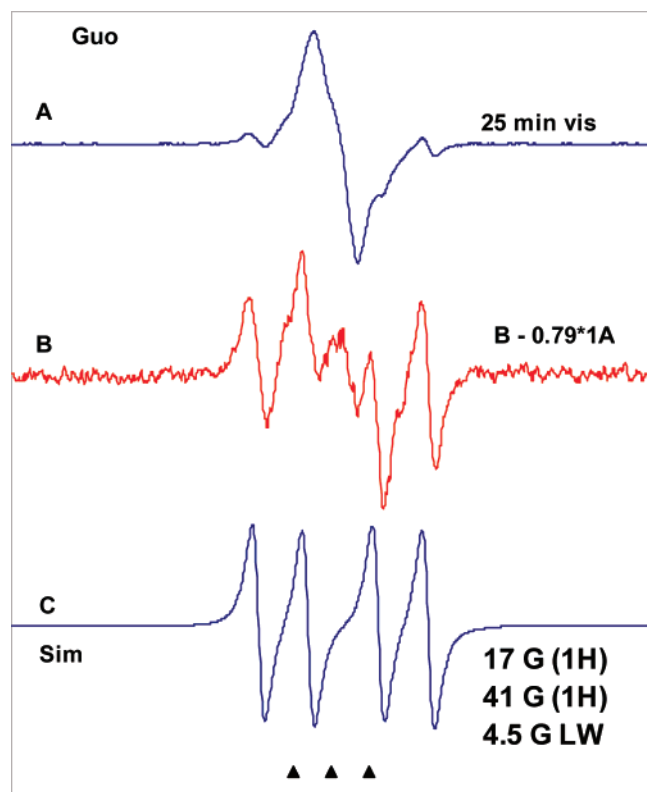


Figure 2. (A) Spectrum of one-electron-oxidized Guo in 7.5 M LiCl/D₂O after visible illumination at 143 K for 25 min showing formation of outer lines of the quartet for C3[•] at the wings. (B) Subtraction (ca. 79%) of the one-electron-oxidized guanine spectrum (spectrum 3G) gives mainly a quartet spectrum ca. 58 G assigned to C3[•] and a doublet ca. 19 G assigned to C5[•]. Spectra A was recorded at 77 K. (C) Spectrum B was simulated using the hyperfine couplings 41 G (1 β H) and 17 G (1 β H) and using a 4.5 G line width and an isotropic *g*-value of 2.0028 (see Table 1). Deuteration at C2'— leads to the loss of the 41 G (1 β H) coupling (see Figure 3D and J and Supporting Information Figure S3).

functional (LYP)¹⁸ and a 6-31-G(d) basis set as implemented in the Gaussian 03 suite of programs.¹⁹ We note that reliable values of isotropic HFCC calculations require an appropriate basis set.²⁰ Recently, Hermosilla et al.²¹ calculated the HFCCs of several molecules in their neutral, cationic and anionic states using the DFT method and different basis sets (6-31G*, TZVP and EPRIII). They have found that the B3LYP/6-31G* method gave HFCCs which are comparable to the experimental values. In our work, we also found that the B3LYP/6-31G* method predicted HFCCs of hydrated guanine radicals in agreement with experiment.⁹

Results

Detection of Sugar Radical Components in Glassy Samples of Guo via Photoexcitation of One-Electron-Oxidized Guanine. In Figures 1A and 2, we present the results of photoexcitation of glassy (7.5 M LiCl/D₂O) samples of Guo via one-electron-oxidized guanine at the natural pH (ca. 5) of the LiCl solution. Figure 1A shows the spectrum of one-electron-oxidized Guo, and Figure 2A shows the spectrum obtained after 25 min of photoexcitation showing formation of sugar radicals as evidenced by developments of extra line components at the center and also at outer lines. Subtraction (ca. 79%) of the one-electron-oxidized guanine spectrum (Figure 1A) from spectrum 2A gives spectrum 2B. This spectrum has a total hyperfine splitting of ca. 58 G, and it shows the line components of a dominant quartet spectrum (C3[•], vide infra). We have simulated

the quartet spectrum of C3[•] (Figure 2C) isotropically using two β -H hyperfine couplings, 17 and 41 G with a line width of 4.5 G. We note that the 17 G coupling (1 β H) is assigned to C4'—H from studies on deuteration at C2'— (see Figure 3D and J and also Supporting Information Figure S3). Less observable in this spectrum are components of a doublet of ca. 19 G (C5[•], vide infra) and an unresolved singlet with a ca. 7.5 G line width (C1[•], vide infra). These become apparent as conditions such as pH and time of irradiation are varied and selective deuteration is employed. Below, we present the results of photoexcitation of one-electron-oxidized guanine in Guo and in its deuterated derivatives at pH 2 and 5 for short irradiation times (Figure 3) and long irradiation times (Figure 4).

Nature of One-Electron-Oxidized Guanine in Guo and Its Deuterated Derivatives at pH ca. 2 and at pH ca. 5. The ESR spectrum of G^{•+} in Guo formed via one-electron oxidation by Cl₂^{•−} in 7.5 M LiCl glass is shown in Figure 3A. The spectrum shown in Figure 3A is identical with those obtained from 1'-D-Guo, 2'-D-Guo and 5',5'-D₂-Guo under similar conditions. We note that the N1 hydrogen in the guanine cation radical (G^{•+}) has a p*K*_a between ca. 5 to 6 in an aqueous (D₂O) glassy environment at low temperatures.⁹ Hence, the spectrum in Figure 3A is of the cation radical, that is, G^{•+} for Guo and similarly for its deuterated derivatives. At the native pH of aqueous (D₂O) 7–7.5 M LiCl glassy systems (ca. 5), the proton at N1 in G^{•+} is over 50% retained. Thus, <50% of the radicals in one-electron-oxidized guanine at the native pH of aqueous (D₂O) 7–7.5 M LiCl glassy systems are in the deprotonated form, G(−H)[•].⁹ Moreover, the ESR spectra of G^{•+} and G(−H)[•] have been observed to be very similar.⁹ The spectrum of one-electron-oxidized guanine in Guo presented in Figure 3G in 7.5 M LiCl glassy systems is therefore a mixture of G^{•+} and G(−H)[•]. This spectrum is identical with those obtained from 1'-D-Guo, 2'-D-Guo, 3'-D-Guo and 5',5'-D₂-Guo under similar conditions, and we have employed it as a benchmark spectrum of one-electron-oxidized guanine for our analyses (Figure 1A).

In our earlier work regarding sugar radical formation via photoexcitation of one-electron-oxidized guanine in dGuo in aqueous (D₂O) 7 M LiCl glassy systems, sugar radical production was found to occur from pH 2 to 6 but is suppressed for pHs above 7.^{2,7} Thus, based on the estimates of p*K*_a of G^{•+} in aqueous (D₂O) 7 M LiCl glassy systems, we concluded that the photoconversion of one-electron-oxidized guanine to sugar radicals was effective for its cation radical (G^{•+}) in dGuo,² in dinucleoside phosphates,^{4,6} DNA-oligomers⁶ and presumably in DNA,^{1,2,6–8} but not for its N1 deprotonated state (G(−H)[•]).² The 2'-deoxyribose or the ribose sugar ring does not have a significant influence on the p*K*_a of G^{•+},^{10,11g,h} and the p*K*_a of G^{•+} in dGuo and in Guo is very close (or nearly identical).^{10,11g,h} In this work, photoexcitation studies at various pHs for Guo show (see Supporting Information Figure S1), as we found for dGuo,² that photoexcitation of one-electron-oxidized guanine is effective in sugar radical production only for the cation radical (G^{•+}) but not for the N1 deprotonated species (G(−H)[•]).

Interpretation of Spectra in Figure 3B–L. In Figure 3B–F, we present the spectra obtained in the glassy samples (7.5 M LiCl in D₂O) in the presence of the electron scavenger K₂S₂O₈ of Guo, 1'-D-Guo, 2'-D-Guo, 3'-D-Guo and 5',5'-D₂-Guo, respectively, at pH ca. 2.0 after appropriate subtraction (ca. 70–82%) of the G^{•+} spectrum from the final spectra obtained after photoexcitation of G^{•+} at 143 K for 25 min. The spectra in Figure 3H–L are obtained for identical samples at pH 5.

The spectra in Figure 3B and H are interpreted as a composite of three major radical species whose benchmark spectra are

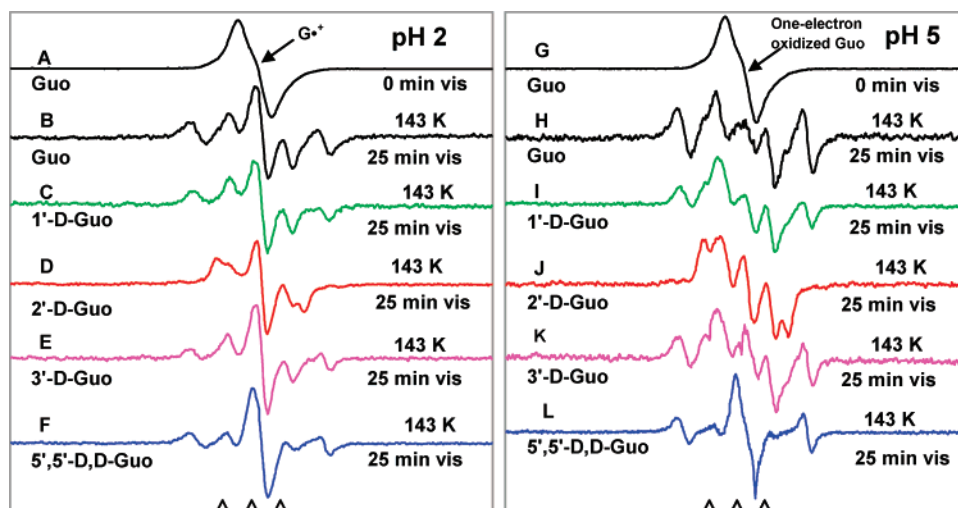


Figure 3. Photoexcitation of one-electron-oxidized guanine in glassy samples of Guo and its deuterated derivatives at pH 2 and 5. Photoexcitation at early time. (left panel) (A) Spectrum of G^{+} in Guo in glassy samples (7.5 M LiCl in D_2O in the presence of the electron scavenger $K_2S_2O_8$) at pH ca. 2 before illumination. Spectra B–F found for sugar radicals formed after photoexcitation for 25 min at 143 K for (B) Guo, (C) 1'-D-Guo, (D) 2'-D-Guo, (E) 3'-D-Guo and (F) 5',5'-D,D-Guo. These spectra were obtained by subtraction of the appropriate amount (ca. 70–82%) of the spectrum of G^{+} (shown in A). (right panel) Spectra taken in the glassy samples at native pH (ca. 5) in 7.5 M LiCl in D_2O in the presence of the electron scavenger $K_2S_2O_8$ of (G) one-electron-oxidized guanine in Guo without photoexcitation at 77 K, of (H) Guo, of (I) 1'-D-Guo, of (J) 2'-D-Guo, of (K) 3'-D-Guo and of (L) 5',5'-D,D-Guo after 25 min of photoexcitation of one-electron-oxidized guanine at 143 K. Each of the spectra H–L was obtained after appropriate subtraction (ca. 70–79%) of the remaining one-electron-oxidized guanine spectrum (G) from the final spectra taken after photoexcitation. All of the spectra were recorded at 77 K.

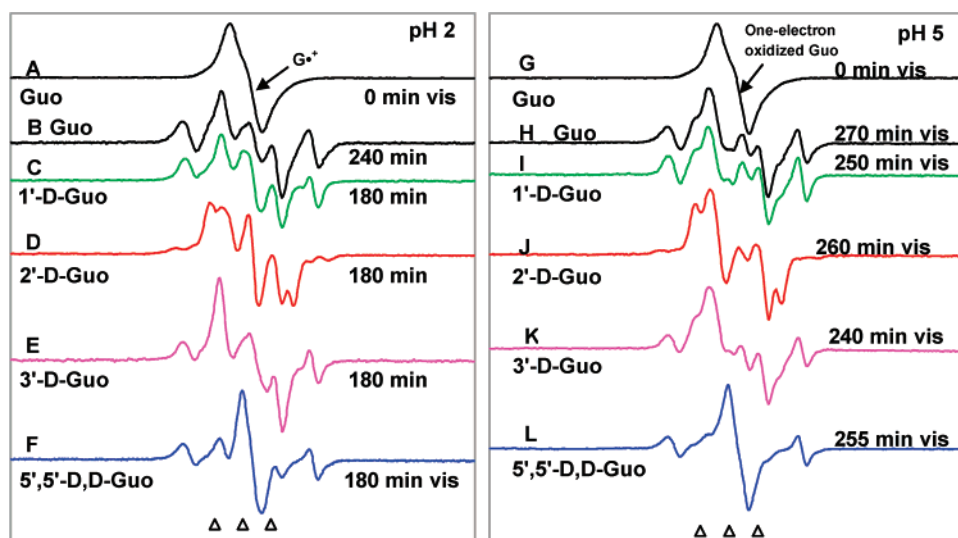


Figure 4. (left panel) (A) Spectrum of G^{+} in Guo in glassy samples (7.5 M LiCl in D_2O in the presence of the electron scavenger $K_2S_2O_8$) at pH ca. 2 before illumination. After appropriate subtraction (ca. 30–36%) of G^{+} (i.e., spectrum A) from the corresponding final spectrum taken after photoexcitation for 180–240 min of photoexcitation at 143 K, we obtain the spectrum for (B) Guo, (C) 1'-D-Guo, (D) 2'-D-Guo, (E) 3'-D-Guo and (F) 5',5'-D,D-Guo. (right panel) Spectra taken in the glassy samples at native pH (ca. 5) in 7.5 M LiCl in D_2O in the presence of the electron scavenger $K_2S_2O_8$ of (G) one-electron-oxidized guanine in Guo without any photoexcitation at 77 K, of (H) Guo, of (I) 1'-D-Guo, of (J) 2'-D-Guo, of (K) 3'-D-Guo and of (L) 5',5'-D,D-Guo after 240–270 min of photoexcitation of one-electron-oxidized guanine at 143 K. Each of the spectra H–L was obtained after appropriate subtraction (ca. 5–15%) of the one-electron-oxidized guanine spectrum (G) from the final spectra taken after photoexcitation. All of the spectra were recorded at 77 K.

shown in Figure 1. They consist of a quartet spectrum of four lines arising from two β -proton couplings in $C3^{\bullet}$ (41 G, 17 G (see Figure 2)), a doublet of 19 G arising from an α -proton coupling in $C5^{\bullet}$ and an unresolved singlet with a ca. 7.5 G line width from $C1^{\bullet}$. The yields of the individual component in the sugar radical cohort vary with pH (Figure 2) and time of photoexcitation (see Supporting Information Figure S2) and allow us to deconvolute the individual radical spectrum. For example, comparing 3B with 3H, we see that in spectrum 3H the singlet from $C1^{\bullet}$ is diminished with increasing pH while the doublet assigned to $C5^{\bullet}$ is increased. This decrease in $C1^{\bullet}$

and augmentation of $C5^{\bullet}$ is found to hold true for the deuterated Guo species as well (compare 3C, 3D and 3E with 3I, 3J and 3K).

Further analysis of the spectra of the deuterated species shown in 3C–F and 3H–L confirms our analysis and assignments.

Spectra for 1'-D-Guo (3C, 3I) are identical to those for Guo (3B, 3H) at corresponding pH values of 2 and 5. This is expected because the $C3^{\bullet}$ and $C5^{\bullet}$ would not show a β -proton coupling at this site. Further, the $C1^{\bullet}$ is formed owing to deprotonation at this site (i.e., at $C1^{\bullet}$); thus, the only effect expected is a deuterium isotope effect on the yield of $C1^{\bullet}$. Such effects have

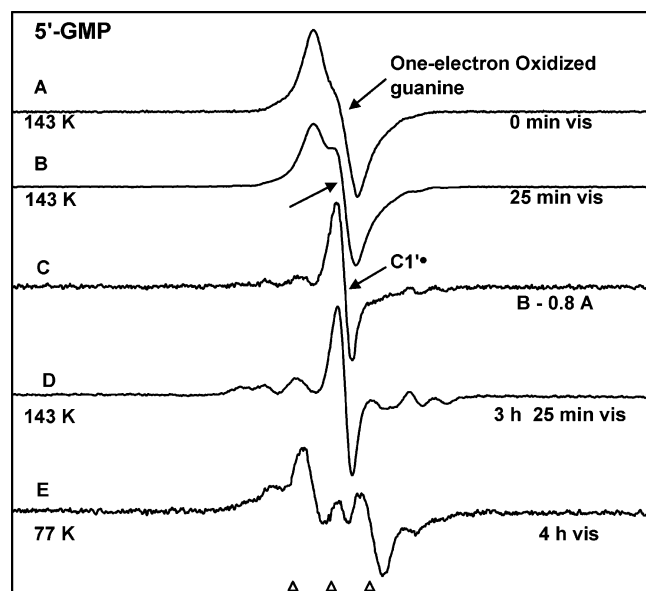


Figure 5. (A) ESR spectrum of one-electron-oxidized guanine in 5'-GMP. (B) Spectrum obtained after photoexcitation for 25 min at 143 K with visible light showing the development of a singlet at the center (indicated by the arrow). (C) Isolation of the singlet after suitable subtraction (ca. 80%) of spectrum 5A from spectrum 5B. This singlet is assigned to $C1^{\bullet}$. (D) Spectrum D is obtained after prolonged photoexcitation, at 143 K, of the same sample used in spectrum B, showing $C1^{\bullet}$ formation (prominent singlet at the center). (E) After photoexcitation at 77 K, of one-electron-oxidized guanine in a fresh sample of 5'-GMP showing predominant formation (ca. 78%) of the doublet ($C5^{\bullet}$) and the line components of the quartet ($C3^{\bullet}$) (ca. 16%) in the wings. Each of the spectra D and E has the appropriate amount (ca. 40% for spectrum D and 60% for spectrum E) of remaining one-electron-oxidized guanine spectrum (part A) subtracted from the final spectra obtained after photoexcitation. The temperatures shown refer to photoexcitation temperatures. All spectra were recorded at 77 K.

been found to be quite small in our previous work with DNA-nucleosides, and little effect is noted in this case as well.² The fact the spectra 3C and 3B as well as 3I and 3H are unaffected on deuteration at $C1'$ —eliminates $C2^{\bullet}$ as a significant contributor, as it would be expected to show a substantial β -proton coupling to the proton at $C1'$ —(Table 1).

The spectra for 2'-D-Guo (3D, 3J) show a loss of the outer lines with new components showing at a total width of 36 G. This is clear evidence that $C3^{\bullet}$ gives rise to the quartet. The deuteration at $C2'$ allows for the assignment of the 41G doublet to the $C2'$ -H proton (see Supporting Information Figure S3).

Spectra for 3'-D-Guo (3E, 3K) are similar to those for Guo (3B, 3H) as well as for 1'-D-Guo (3C, 3I) as they show identical hyperfine splittings, although the relative amounts of the individual radicals in the cohort vary slightly. This is expected, since the $C1^{\bullet}$, $C3^{\bullet}$ and $C5^{\bullet}$ would not show a β -proton coupling at this site. Only $C2^{\bullet}$ and $C4^{\bullet}$ would be expected to show change in hyperfine splittings, and the lack of these changes shows these species are not formed in observable amounts. The formation of the $C3^{\bullet}$ occurs via deprotonation at the $C3'$ site; as a consequence, we expect a deuterium isotope effect on the yield of $C3^{\bullet}$ in 3'-D-Guo. Such effects have been found to be small in our previous work with DNA-nucleosides,² and we do find a modest reduction in the yield of $C3^{\bullet}$ and increases in the relative amounts of $C1^{\bullet}$ and $C5^{\bullet}$ (compare 3B with 3E).

The spectra for 5',5'-D,D-Guo (3F, 3L) clearly show the loss of the 19 G doublet and an increase in the size of the central component on deuteration. Thus, we can assign unequivocally

the doublet to the $C5^{\bullet}$. Again, we noted little evidence for a significant deuterium isotope effect in the formation of the $C5^{\bullet}$. Similar results were previously found for the DNA analogue 5',5'-D,D-dGuo.² On deuteration at $C5'$, the quartet spectrum remains in spectra 3F and 3L, as expected for $C3^{\bullet}$.

Photoexcitation for Extended Times. On photoexcitation for extended time periods, $C1^{\bullet}$ is lost and $C5^{\bullet}$ is found to increase. In Figure 4B–F, we present the ESR spectra of sugar radicals formed via photoexcitation of G^{+} in glassy samples of Guo and of its deuterated derivatives at pH ca. 2 after 180–240 min of photoexcitation. In Figure 4H–L, the corresponding ESR spectra are shown for these glassy samples at the native pH (ca. 5) of 7.5 M LiCl in D_2O .

Comparing Figures 3 and 4, we find that the relative amounts of $C1^{\bullet}$, $C3^{\bullet}$ and $C5^{\bullet}$ were dependent on the length of photoexcitation. While photoexcitation gradually removes $C1^{\bullet}$, even at pH ca. 2 at these longer times we observe some remaining singlet from $C1^{\bullet}$. The important difference between the early and late photoexcitation in these samples is the predominant formation of $C5^{\bullet}$ (see spectra 4H–K). Plots of the change in radical intensities with time are given in the Supporting Information (Figure S2), and details of the analyses are shown in Figure S4.

Photo-oxidation of One-Electron-Oxidized Guanine in 5'-GMP. In Figure 5A, we show the ESR spectrum of one-electron-oxidized guanine (77 K) from 5'-GMP produced via one-electron oxidation by $Cl_2^{\bullet-}$. This spectrum is identical with that shown in Figure 3G for guanosine. Figure 5B shows the spectrum after 25 min of photoexcitation at 143 K, indicating formation of a singlet at the center apart from other line components.

Suitable subtraction (ca. 80%) of spectrum 5A from spectrum 5B isolates the singlet, as represented in Figure 5C, and we assign the singlet to $C1^{\bullet}$. While this species dominates the spectrum, one can also see small line components in the wings that are due to a quartet as well as other line components that extend up to ca. 66 G. After continued photoexcitation of this same sample at 143 K for 3 h more, spectrum 5D is observed showing the formation of this singlet (i.e., production of $C1^{\bullet}$) and the line components of the quartet and outermost line components that extending to ca. 66 G become more prominent. About 60% of one-electron-oxidized guanine is converted to sugar radicals. We assign tentatively the quartet as $C3^{\bullet}$ and line components having total hyperfine splitting with ca. 66 G as $C4^{\bullet}$ from a comparison to literature results for $C4^{\bullet}$ in an irradiated single crystal of inosine.²²

An identically prepared glassy sample of one-electron-oxidized 5'-GMP was photoexcited for 4 h at 77 K and the corresponding spectrum is presented in Figure 5E showing 40% of one-electron-oxidized guanine is converted to sugar radicals. The sugar radicals are dominated by $C5^{\bullet}$ (ca. 78%) with smaller contributions estimated from $C1^{\bullet}$ (ca. 6%) and $C3^{\bullet}$ (ca. 16%). For analysis of line components of $C3^{\bullet}$ in glassy samples of 5'-GMP at 77 K, we have used a simulated spectrum for $C3^{\bullet}$ having two β -hydrogen hyperfine couplings of 30 and 14 G using a 5 G line width and these couplings agree with the theoretical prediction very well (see Table 1 and Supporting Information Figures S5–S8). We note that these couplings for $C3^{\bullet}$ are different in 5'-GMP samples in comparison to their corresponding values for Guo samples. This observation, as we have already mentioned in the Materials and Methods section, is consistent with our earlier works for couplings of $C3^{\bullet}$ in dGuo at 143 K,² 5'-dGMP at 77 K² and in 5'-dAMP samples at 143 K.³

SCHEME 3: Radicals Considered in This Work

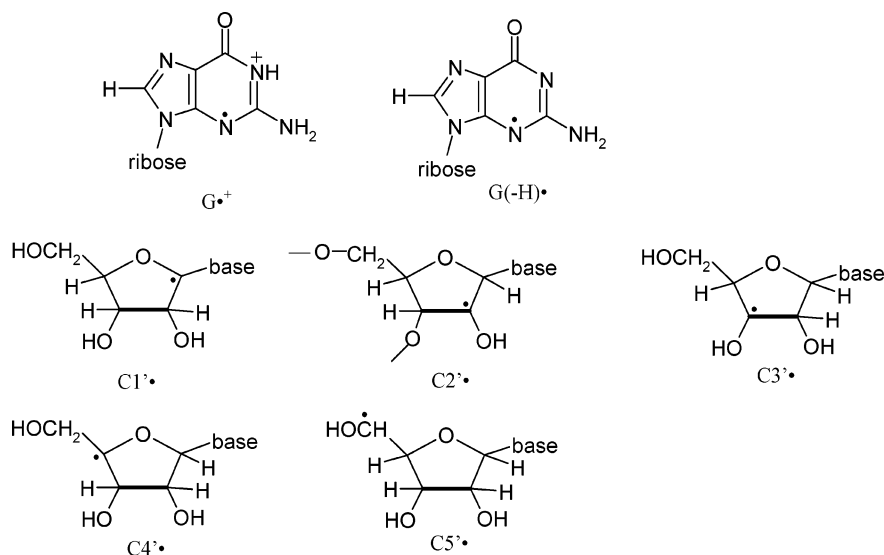


TABLE 1: Hyperfine Couplings (HFCCs) and *g*-Values for Ribose Radicals Observed Experimentally in RNA^a (Theoretical HFCCs Are Calculated Using the B3LYP/6-31G* Method)

radical ^b	compound	hyperfine coupling constant (HFCC)/G	<i>g</i> -value (apparent) ^c
C1•	5'-GMP, RNA-oligo	singlet (7.5 G line width)	2.0027
C3•	Guo	41 (β C2'H), ^d 17 (β C4'H) ^d	2.0028
C5•	Guo	(-)19 (C5'αH)	2.0025
doublet	RNA-oligo	28	2.0031

^{a,b} Values are for radicals formed via photoexcitation at 143 K in the frozen aqueous (7.5 M LiCl D₂O) glassy solution with native pH (ca. 5). These values are obtained from the spectra recorded at 77 K. ^c The apparent *g*-value is the experimental center of the spectrum. ^d This assignment is done based on Supporting Information Figure S3.

In summary, photoexcitation of one-electron-oxidized 5'-GMP shows primarily C1• formation at 143 K and predominantly C5• with small amounts of C1• and C3• at 77 K. These results are very similar to the corresponding results of photoexcitation of one-electron-oxidized guanine in glassy samples of 5'-dGMP at 143 K and at 77 K.² In 5'-dGMP, photoexcitation of one-electron-oxidized guanine at 143 K produces C1• almost exclusively, whereas, at 77 K, the distribution of various sugar radicals in the cohort was C1• (ca. 15%), C3• (30%) and C5• (ca. 55%).²

Photoexcitation of One-Electron-Oxidized Guanosine in RNA-Oligomers. In Figure 6A, we show the ESR spectrum of one-electron-oxidized RNA-oligomer UGGGU, formed via one-electron oxidation by Cl₂⁻ in a 7.5 M LiCl glass in D₂O in the presence of the electron scavenger K₂S₂O₈. This spectrum and those of one-electron-oxidized UAGAU, UUGGUU, UUCGAA and UCGCU are found to be to that of predominantly one-electron-oxidized guanine (see Supporting Information Figure S9 as well as Figure 3G for Guo).

Figure 6B shows the spectrum obtained after photoexcitation of one-electron-oxidized guanine in UGGGU at 143 K for 35 min. Careful subtraction (ca. 75%) of spectrum A from spectrum B shows spectrum C having a singlet (identical with that in Figure 5C for 5'-GMP samples), that is, C1• (ca. 35%) and a doublet of ca. 28 G (ca. 65%). In Figure 6D, the spectrum found after extended photoexcitation (ca. 185 min) is shown (60% of spectrum 6A was subtracted to show only the photoproduct). Here, we find that the relative amount of the singlet (i.e., C1•) is ca. 20% and that of the doublet is ca. 80%. The change in

relative contributions of the two species (C1• and 28 G doublet) with photoexcitation suggests the C1• is unstable to photoconversion to the doublet species.

The other RNA-oligomers used in this study, namely, UAGAU, UUGGUU, UUCGAA and UCGCU, were prepared in the same way as UGGGU, that is, in 7.5 M LiCl glass in D₂O in the presence of the electron scavenger K₂S₂O₈. Like the UGGGU sample, these glassy samples were all γ -irradiated, annealed to form one-electron-oxidized guanine and subsequently photoexcited for 185 min at 143 K. These samples also show formation of the singlet (C1•) and the "doublet" of ca. 28 G via photoexcitation in different proportions (see Supporting Information Figure S10). As found for UGGGU, the C1• and the "doublet" of ca. 28 G in all of these RNA-oligomers were isolated via the subtraction of the one-electron-oxidized guanine spectrum from the final spectra obtained after illumination. We also note that, in these RNA-oligomers, in addition to C1• and the "doublet" formation, we find other line components in the wings which are most probably from an impurity. Protecting groups used during the synthesis of the RNA-oligomer are found to produce similar line components (see Supporting Information Figure S10).

For the RNA-oligomer UUGGUU, we did not find strong evidence for formation of C5• after photoexcitation at 143 K or at 77 K (see Supporting Information Figure S11). Also, we note that, similar to our observation in the case of RNA-oligomer samples at 143 K, the relative contributions of singlet (i.e., C1•) and "doublet" favor the formation of the doublet with extended photoexcitation at 77 K (see Supporting Information Figures S11–S14).

Theoretical Studies. It is well-established that sugar radicals are able to take on a variety of conformations that are described by the pseudorotation cycle. In aqueous media, the relative stabilities of these various conformations will not only depend on the internal geometry considerations but will also be affected by hydrogen bonding both internally and to the solvent.¹³ Therefore, in this study, we sought those conformations (Figure 7) giving hyperfine coupling constants (HFCCs) close to the experimental values.

The crystal structures of nucleosides and nucleotides²³ and solution phase NMR studies^{24–29} suggest that the conformation of the sugar ring can be adequately described by two conformations such as the C3'-endo-C2'-exo (North sugar) and C2'-endo-

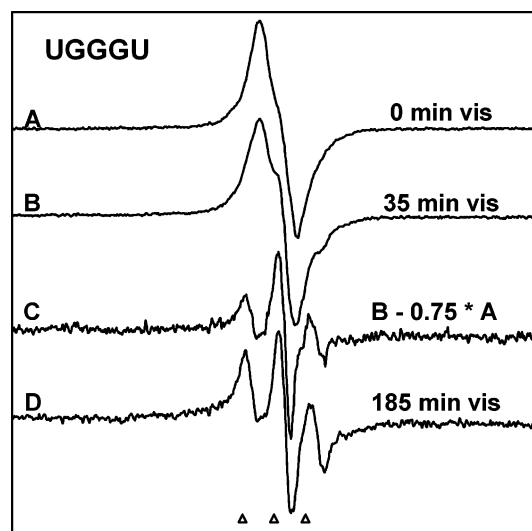


Figure 6. (A) Spectrum A shows the one-electron-oxidized guanine formed in a RNA-oligo, UGGGU, via one-electron oxidation by $\text{Cl}_2^{\bullet-}$ in a 7.5 M LiCl glass in D_2O in the presence of the electron scavenger $\text{K}_2\text{S}_2\text{O}_8$ after annealing for 10 min at 152 K in the dark. (B) Spectrum B shows the result of visible photoexcitation of this sample for 35 min at 143 K. (C) In spectrum C, we show the result of subtraction of 0.75 of spectrum A from the spectrum showing the formation of the singlet (C1^\bullet) ca. 35% and the doublet ca. 28 G (65%). (D) Spectrum D is obtained by subtraction of ca. 60% of spectrum A from the spectrum recorded after further photoexcitation (total 185 min) at 143 K. All of the spectra were recorded at 77 K.

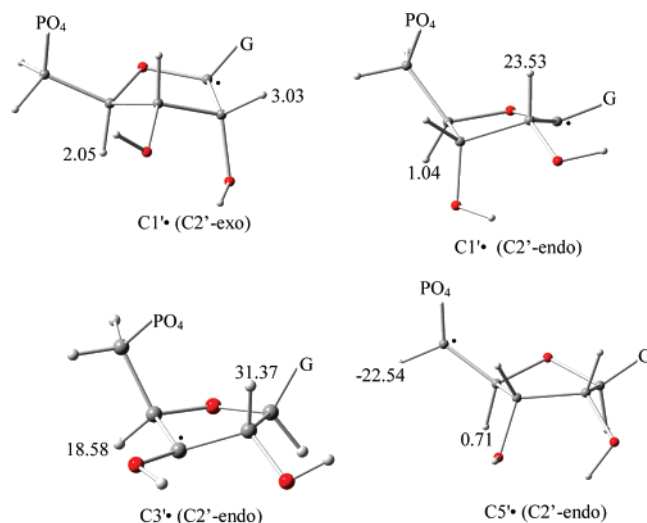


Figure 7. B3LYP/6-31G* optimized different radicals that were generated from 5'-GMP cation radical, respectively. For clarity, the guanine base and PO_4 group are not shown in structural detail. HFCC values are mentioned in Gauss (G).

$\text{C3}'\text{-exo}$ (South sugar) equilibrium models.¹³ It was also found that the energy barrier between the two conformations varies between ca. 1.2 and 5.0 kcal/mol.^{30,31} Therefore, in the present study, initial geometries of 5'-GMP cation radical were generated in $\text{C2}'\text{-endo-C3}'\text{-exo}$ ($\text{C2}'\text{-endo}$) and $\text{C3}'\text{-endo-C2}'\text{-exo}$ ($\text{C2}'\text{-exo}$) conformations and were fully optimized using the B3LYP/6-31G* method. The 5'-GMP cation radical is found to be more stable (~ 4.0 kcal/mol) in the $\text{C2}'\text{-endo}$ conformation than the corresponding $\text{C2}'\text{-exo}$ conformation (see Supporting Information Figure S5). Further, different sugar radicals (C1^\bullet , C2^\bullet , C3^\bullet , C4^\bullet and C5^\bullet) were generated by abstracting the corresponding hydrogen atom from the sugar moiety of 5'-GMP cation radical starting in their $\text{C2}'\text{-endo}$ and $\text{C2}'\text{-exo}$ conformations, respec-

tively (see Supporting Information Figures S6–S8). The geometries of these sugar radicals were optimized and hyperfine coupling constants (HFCCs) were calculated using the same method and basis set.

In Table 2, we present the HFCCs of the various sugar radicals as calculated using the B3LYP/6-31G* method along with their experimental HFCCs.

C1^\bullet . Experimentally, we have assigned a singlet ($< \text{ca. } 4$ G) to C1^\bullet in both nucleotides, for example, 5'-GMP, and in RNA-oligomers (see Figures 5 and 6). We have observed formation of this singlet in Guo at low pH (ca. 2) (see Figure 3). B3LYP/6-31G* calculated HFCCs of C1^\bullet in $\text{C2}'\text{-exo}$ conformation show two small couplings at $\text{C2}'\text{-H}$ and at $\text{C4}'\text{-H}$ sites having values of ca. 3.0 and 2.1 G, respectively. However, the $\text{C2}'\text{-endo}$ conformation gives substantial HFCCs (ca. 23.5 G) for C1^\bullet at $\text{C2}'\text{-H}$ and a very small coupling of ca. 1 G at $\text{C4}'\text{-H}$. Clearly, experimental results suggest that, for C1^\bullet , the $\text{C2}'\text{-exo}$ conformer dominates (see Table 2). From the HFCC values, we note that the 28 G doublet found in the oligonucleotides might be C1^\bullet in the $\text{C2}'\text{-endo}$ form.

C2^\bullet . HFCCs of C2^\bullet obtained using the B3LYP/6-31G* method in the $\text{C2}'\text{-exo}$ conformation show two couplings at $\text{C1}'\text{-H}$ and at $\text{C3}'\text{-H}$ sites of ca. 13.8 and 24.0 G, respectively. The corresponding HFCCs of C2^\bullet starting in $\text{C2}'\text{-endo}$ give HFCC values of 18.8 G at $\text{C1}'\text{-H}$ and 28.0 G at $\text{C3}'\text{-H}$. However, close analyses of the conformations of the ribose ring for both the $\text{C2}'\text{-exo}$ and $\text{C2}'\text{-endo}$ conformations correspond to the $\text{C2}'\text{-exo}$ form. These results indicate that C2^\bullet should be a quartet having a total hyperfine splitting of ca. 38 G to ca. 47 G. ESR spectral studies using samples of 1'-D-Guo and 3'-D-Guo show that we have not found any observable signature of C2^\bullet formation in Guo (see Figures 3 and 4 and Supporting Information Figure S4). Moreover, in RNA-oligomers, we have not observed a quartet that would suggest this radical species; however, the 28 G doublet found in oligos is a possibility.

C3^\bullet . ESR spectral studies using Guo and its deuterated derivatives (at $\text{C1}'\text{-}$, $\text{C2}'\text{-}$, $\text{C3}'\text{-}$ and at $\text{C5}'\text{-}$) have aided in assignment of the couplings of C3^\bullet in Guo (see Figures 3 and 4 and also Supporting Information Figure S3) as ca. 41 G (at $\text{C2}'\text{-H}$) and ca. 17 G (at $\text{C4}'\text{-H}$). The calculated HFCCs of C3^\bullet in Guo in $\text{C2}'\text{-endo}$ and in $\text{C2}'\text{-exo}$ conformations are found to be ca. 31.9 G at $\text{C2}'\text{-H}$ and 20.9 G at $\text{C4}'\text{-H}$ and ca. 8.1 G at $\text{C2}'\text{-H}$ and 29.2 G at $\text{C4}'\text{-H}$, respectively (see Figure 8). The corresponding values of HFCCs for C3^\bullet in 5'-GMP are ca. 31.4 G at $\text{C2}'\text{-H}$ and 18.6 G at $\text{C4}'\text{-H}$ and ca. 10.7 G at $\text{C2}'\text{-H}$ and 26.9 G at $\text{C4}'\text{-H}$, respectively (see Supporting Information Figures S7 and S8). We note here that, in 5'-GMP systems after long photoexcitation times (4 h) (see Figure 5E), line components suggest formation of C3^\bullet with HFCCs ca. 30 and 14 G and this is in good agreement for the optimized structure of C3^\bullet in $\text{C2}'\text{-exo}$ in 5'-GMP for which we find 26.9 G at $\text{C2}'\text{-H}$ and 10.7 G at $\text{C4}'\text{-H}$ (see Supporting Information Figure S7).

C4^\bullet . We have obtained HFCCs of C4^\bullet employing the B3LYP/6-31G* method in $\text{C2}'\text{-exo}$ as well as in $\text{C2}'\text{-endo}$ conformations. The calculations show that, in the $\text{C2}'\text{-exo}$ conformation, C4^\bullet has the largest HFCC at $\text{C3}'\text{-H}$ (28.3 G) and a considerable one at the $\text{C5}'\text{-H}$ site (8.1 G) as well as two small couplings of ca. 1.7 G at the remaining $\text{C5}'\text{-H}$ and ca. 0.3 G at $\text{C1}'\text{-H}$. On the other hand, in the $\text{C2}'\text{-endo}$ conformation, theoretical calculations show all small couplings of ca. 2.9 G ($\text{C1}'\text{-H}$), 7.3 G ($\text{C3}'\text{-H}$), 5.1 and 2.2 G ($\text{C5}'\text{-H}$) sites. We also note that theoretical predictions regarding the

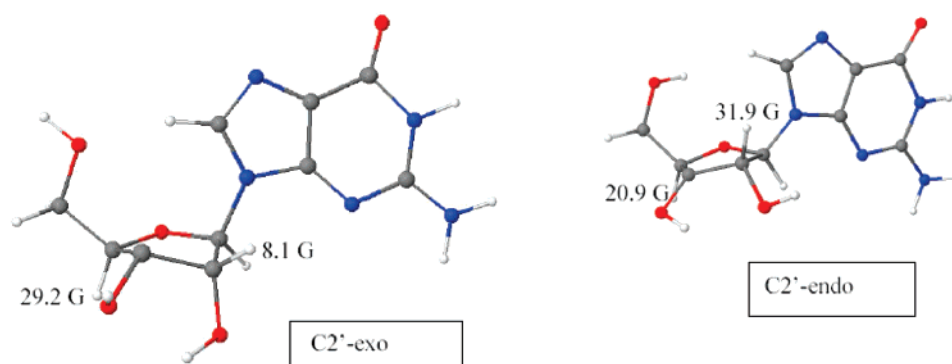


Figure 8. B3LYP/6-31G* optimized geometries of C3• in Guo in two conformations.

TABLE 2: Hyperfine Couplings (HFCCs) and *g*-values for Ribose Radicals in RNA (Theoretical HFCCs Are Calculated Using the B3LYP/6-31G* Method)

name of the radical	compound ^a	hyperfine coupling constants (G)			
		site	theory ^b		experiment ^c
			C2'-endo	C2'-exo	
C1•	5'-GMP	β(C2'H)	23.5	3.0	singlet
		δ(C4'H)	1.0	2.1	ca. 7.5 G line width
C2•	5'-GMP	β(C1'H)	18.8	13.8 ^d	not identified
		β(C3' H)	28.0	24.0 ^d	
C3•	Guo	β(C2' H)	31.9	8.1	ca. 41 (βC2'H)
		β(C4' H)	20.9	29.2	ca. 17 (βC4'H)
	5'-GMP	β(C2' H)	31.4	10.7	
		β(C4' H)	18.6	26.9	<i>e</i>
C4•	5'-GMP	δ(C1' H)	2.9	0.3	not identified
		β(C3' H)	7.3	28.3	
		β(C5' H)	5.1	1.7	
		β(C5' H)]	2.2	8.1	
C5•	5'-GMP	α(C5' H)	−22.45	−21.6	ca. −19 G (αC5' H)
		β(C4' H)]	0.7	0.6	

^a Compounds employed to obtain the HFCC values theoretically. ^b HFCCs of different sugar radicals were calculated with starting geometries in the C2'-endo and C2'-exo conformations (see Supporting Information Figures S6–S8). ^c The experimentally found HFCCs were taken from Table 1. ^d For C2•, the corresponding HFCCs of C2• starting in the C2'-exo conformation optimize to the C2'-endo form, resulting in similar couplings (see Supporting Information Figure S6). ^e We found line components (Figure 5E) suggesting the following couplings: 14 G (1 β H) and 30 G (1 β H).

dependence of HFCC of C4• with respect to the pseudorotation cycle have been attempted^{13b} to match the existing experimental (single crystal EPR/ENDOR) data.²² For example, recently, Parr and Wetmore^{13c} have shown that the sugar radicals (e.g., C4• in DNA) can adopt numerous conformations within ca. 9 kcal/mol using the B3LYP/6-31G(d,p) method.

C5•. The collapse of the central doublet of ca. 19 G in 5',5'-D,D-Guo (see Figures 3 and 4) gives an unequivocal signature of C5• in Guo. Also, observation of a similar doublet (ca. 19 G) during photoexcitation in 5'-GMP samples at 77 K (see Figure 5E) suggests formation of C5•. Theoretically, we find that either of the C2'-endo or of the C2'-exo conformations give an α -H HFCC of ca. -22 G at C5'-H with only a small coupling from the β -proton at C4' (0.7 G).

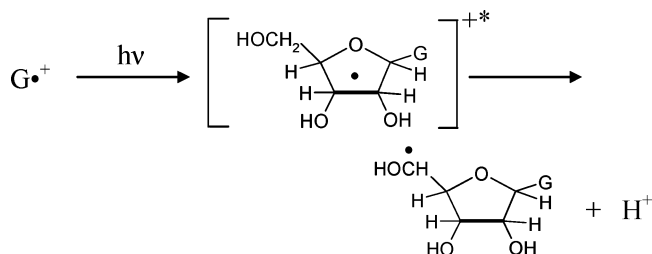
Discussion

Identities of the Sugar Radicals Formed in RNA-Nucleosides via Photoexcitation of One-Electron-Oxidized Guanine.

The results reported in this work clearly show that C1•, C3• and C5• sugar radicals are produced in Guo on photoexcitation of one-electron-oxidized guanine and their relative amounts vary with pH and length of photoexcitation time. As with our work with dGuo,² deuteration at selective sites in Guo helps us in assigning the radical site in Guo. For example, in 2'-D-Guo, collapse of the line components of ca. 41 G in spectra 3D, 3J,

4D and 4J shows that the quartet is due to C3•. Similarly, in 5',5'-D,D-Guo, collapse of the central doublet of ca. 19 G in spectra 3F, 3L, 4F and 4L establishes that the ca. 19 G doublet is due to C5•. The central singlet observed in spectra 3B–F and in 4B–F in Guo derivatives at pH ca. 2 is assigned to C1•.

In addition to these deuteration studies, we have justified our assignments on the basis of theoretical calculations. We have considered both C2'-exo and C2'-endo conformations of the sugar radicals. Each of these radical species has a significant and varying degree of nonplanarity (see Figures 7 and 8 and also Supporting Information Figures S6–S8). The HFCC values in Table 2 clearly show that C1• in the C2'-exo conformation clearly gives a singlet; that is, for C1•, the C2'-exo conformation is favored. For C5•, both the C2'-exo and C2'-endo conformations give similar couplings; that is, for C5•, we do not note any preference in conformation. For C3•, we find that the equilibrium gas phase geometry in the C2'-endo conformation does account qualitatively for the experimentally observed couplings. However, to reproduce the experimentally observed HFCCs of C3• using theoretical calculations, we suggest that solvent induces a geometry of C3• in the C2'-endo conformation that produces the larger hyperfine coupling. This is not unexpected, since solvent water hydrogen bonding clearly can stabilize other conformations.

SCHEME 4: Formation of a Sugar Radical, e.g., C5'•, via Photoexcited G^{•+}


The driving forces for the site of formation of the sugar radicals are of interest. The small deuterium isotope effect found for 3'-D-Guo and 5',5'-D₂-Guo suggests that the transition state for deprotonation is very similar to the geometry of the excited state of the radical cation. Further, the relative bond C—H bond energies in the sugar ring are not found to control the site of the deprotonation. It is the charge and spin density at each site in the ring in the excited state that accounts for the site of deprotonation.^{2,7} The conformation of the sugar ring likely affects this charge-spin distribution, and this is under study. In addition, the availability of proton acceptor sites is also an important consideration in the determination of the site of deprotonation.^{2,7,8}

Effect of Phosphate Substitution. In previous works employing 3'-dGMP and 5'-dGMP² and 3'-dAMP and 5'-dAMP,³ we found that the presence of phosphate at C5' resulted in deactivation of formation of C5'•. This was supported by our theoretical calculations.^{13a,32} In agreement with this past work, experimental results for the photoexcitation of G^{•+} in 5'-GMP at 143 K (Figure 5C) show the dominant singlet of C1'• and formation of C5'• to a much smaller extent. However, we do not find a hindrance to C5'• formation at 77 K. For photoexcitation at 77 K, we find the 19 G doublet due to C5'• (see Figure 5E) dominates the spectrum. This same phenomenon was found in our work regarding photoexcitation of one-electron guanine in 5'-dGMP samples at 77 K², that is, a dramatic change in radical formation from C1'• at 143 K to C5'• at 77 K. These results suggest that molecular relaxation of the excited cation radical allowed at the warmer temperature likely changes the site of deprotonation in the sugar moiety.^{2,3,6–8} Thus, at 77 K, this process is kinetically driven as molecular relaxation is not possible, while, at 143 K, relaxation allows the thermodynamics of the relative bond energies to come into play. The recent experimental finding showing decrease of excited-state intramolecular proton transfer with increasing viscosity in protic media³³ also supports this proposition.

Identities of Sugar Radicals Formed in RNA-Oligomers via Photoexcitation of One-Electron-Oxidized Guanine. The spectra shown in Figure 6 indicate that mainly two types of sugar radicals are produced in RNA-oligomers via photoexcitation of one-electron-oxidized guanine—the singlet at the center (C1'•) and the doublet ca. 28 G. The relative amounts of the two radicals vary with time of photoexcitation: Initially, formation of the 28 G doublet is favored only slightly. However, upon extended photoexcitation, the 28 G doublet dominates (see Figure 6). This observation suggests a conversion of C1'• to the 28 G doublet. Our theoretical calculations suggest that this doublet ca. 28 G could either be C1'• in the C2'-endo conformation (see Table 2 and Figure 7), C4'• in the C2'-exo conformation (see Table 2 and Supporting Information), or finally C2'• could account for this coupling provided the theoretically predicted β -H coupling at C1' (18.8 G, see Table

2) is substantially smaller (say ca. ≤ 7 G). Further experimental work is ongoing in our laboratory to assign this doublet.

Conclusion

This work shows that formation of specific neutral sugar radicals occurs via photoexcitation of guanine cation radical (G^{•+}) in RNA-nucleosides, -nucleotides, and -oligomers. We conclude the mechanism of neutral sugar formation via photoexcitation of base cation radicals in DNA is valid for RNA systems as well (see Scheme 4).

Acknowledgment. This work was supported by the NIH NCI under Grant No. R01CA045424. A.K. and M.D.S. are thankful to Arctic Region Supercomputing center (ARSC) for a generous grant of CPU time and facilities. A.K. is personally thankful to the ARSC staff for their constant co-operation and timely help. We are grateful to Omicron Biochemicals Inc. for timely syntheses of the deuterated Guo derivatives employed in this work.

Supporting Information Available: Supporting information is available and includes the following. Figure S1 shows results of photoexcitation of one-electron-oxidized Guo as a function of pH. Figure S2 plots the extent of formation of various sugar radicals with time at pHs of ca. 2 and ca. 5 via photoexcitation of one-electron-oxidized Guo at 143 K. Figure S3 shows that, for C3'• in 2'-D-Guo samples, the resulting spectrum is best predicted by the replacement of the 41 G hyperfine coupling with a deuterium coupling of 6.3 G. Figure S4 shows the analyses and the sugar radical cohort at various times of photoexcitation for glassy samples of 3'-D-Guo at pH ca. 2. Figure S5 showing optimized geometries of 5'-GMP cation radical in C2'-exo and C2'-endo conformations. Figure S6 presents the optimized geometries of various sugar radicals in 5'-GMP. Figure S7 presents the optimized geometries of various sugar radicals in the C2'-exo conformation. Figure S8 shows the optimized geometries of various 5'-GMP sugar radicals in the C2'-endo conformation. Figure S9 representing ESR spectra of one-electron-oxidized UGGGU, UAGAU, UUGGUU, UUCGAA and UCGCU shows that each one of these spectra predominantly results from G^{•+}. Figure S10 shows the formation of C1'• and the doublet ca. 28 G via photoexcitation of one-electron-oxidized guanine in various RNA-oligomers (UAGAU, UUGGUU, UUCGAA and UCGCU). Figure S11 shows photo-oxidation of one-electron-oxidized UUGGUU at 77 K leading to the sugar radical formation (mainly C1'• and the doublet ca. 28 G). Figures S12–S14 show the extent of formation of C1'• and the “doublet” of ca. 28 G via photoexcitation of one-electron-oxidized guanine at 143 K with time in UCGCU, UUGGUU and UGGGU, respectively. This material is available free of charge via the Internet at <http://pubs.acs.org>.

References and Notes

- (1) Shukla, L. I.; Pazdro, R.; Huang, J.; DeVreugd, C.; Becker, D.; Sevilla, M. D. *Radiat. Res.* **2004**, *161*, 582–590.
- (2) Adhikary, A.; Malkhasian, A. Y. S.; Collins, S.; Koppen, J.; Becker, D.; Sevilla, M. D. *Nucleic Acids Res.* **2005**, *33*, 5553–5564.
- (3) Adhikary, A.; Becker, D.; Collins, S.; Koppen, J. and Sevilla, M. D. *Nucleic Acids Res.* **2006**, *34*, 1501–1511.
- (4) Adhikary, A.; Kumar, A.; Sevilla, M. D. *Radiat. Res.* **2006**, *165*, 479–484.
- (5) Kumar, A.; Sevilla, M. D. *J. Phys. Chem. B* **2006**, *110*, 24181–24188.
- (6) Adhikary, A.; Collins, S.; Khanduri, D.; Sevilla, M. D. *J. Phys. Chem. B* **2007**, *111*, 7415–7421.
- (7) (a) Becker, D.; Adhikary, A.; Sevilla, M. D. In *Charge Migration in DNA Physics, Chemistry and Biology Perspectives*; Chakraborty, T., Ed.;

- Springer-Verlag: Berlin, Heidelberg, 2007; pp 139–175. (b) Becker, D.; Adhikary, A.; Sevilla, M. D. In *Recent Trends in Radiation Chemistry*; Rao, B. S. M., Wishart, J., Eds.; World Scientific Publishing Co.: Singapore, New Jersey, London, 2007 (in press).
- (8) Kumar, A.; Sevilla, M. D. In *Radiation Induced Molecular Phenomena in Nucleic Acid: A Comprehensive Theoretical and Experimental Analysis*; Shukla, M. K., Leszczynski, J., Eds.; Springer-Verlag: Berlin, Heidelberg, New York, 2007 (in press).
- (9) Adhikary, A.; Kumar, A.; Becker, D.; Sevilla, M. D. *J. Phys. Chem. B* **2006**, *110*, 24171–24180 and references therein.
- (10) (a) Candeias, L. P.; Steenken, S. *J. Am. Chem. Soc.* **1989**, *111*, 1094–1099. (b) Steenken, S. *Chem. Rev.* **1989**, *89*, 503–520. (c) Steenken, S. *Free Radical Res. Commun.* **1992**, *16*, 349–379. (d) Burrows, C. J.; Muller, J. G. *Chem. Rev.* **1998**, *98*, 1109–1152. (e) Reynisson, J.; Steenken, S. *Phys. Chem. Chem. Phys.* **2001**, *4*, 527–532.
- (11) (a) Becker, D.; Sevilla, M. D. *Adv. Radiat. Biol.* **1993**, *17*, 121–180. (b) Becker, D.; Sevilla, M. D. In *Royal Society of Chemistry Specialist Periodical Report*; Gilbert, B. C., Davies, M. J., Murphy, D. M., Eds.; *Electron Spin Resonance*. **1998**, *16*, 79–114. (c) Weiland, B.; Hüttermann, J. *Int. J. Radiat. Biol.* **1998**, *74*, 341–358 and references therein. (d) Weiland, B.; Hüttermann, J. *Int. J. Radiat. Biol.* **1999**, *75*, 1169–1175 and references therein. (e) Ward, J. F. *Cold Spring Harbor Symp. Quant. Biol.* **2000**, *65*, 377–382 and references therein. (f) Sevilla, M. D.; Becker, D. In *Royal Society of Chemistry Specialist Periodical Report*; Gilbert, B. C., Davies, M. J., Murphy, D. M., Eds.; *Electron Spin Resonance*. **2004**, *19*, 243–278. (g) Bernhard, W. A.; Close, D. M. In *Charged Particle and Photon Interactions with Matter Chemical, Physicochemical and Biological Consequences with Applications*; Mozumdar, A., Hatano, Y. Eds.; Marcel Dekker, Inc.: New York, Basel, 2004; pp 431–470. (h) von Sonntag, C. *Free-radical-induced DNA Damage and Its Repair*; Springer-Verlag: Berlin, Heidelberg, 2006; pp 335–447.
- (12) (a) Altona, C.; Sundaralingam, M. *J. Am. Chem. Soc.* **1972**, *94*, 8205–8212. (b) Altona, C.; Sundaralingam, M. *J. Am. Chem. Soc.* **1973**, *95*, 2333–2344. (c) Sanger, W. *Principles of Nucleic Acid Structure*; Springer-Verlag: New York, 1984.
- (13) (a) Colson, A.-O.; Sevilla, M. D. *J. Phys. Chem.* **1995**, *99*, 3867–3874. (b) Guerra, M. *Res. Chem. Intermed.* **2002**, *28*, 257–264. (c) Parr, K. D.; Wetmore, S. D. *Chem. Phys. Lett.* **2004**, *389*, 75–82. (d) Khoroshun, D. V.; Warncke, K.; Ke, S.-C.; Musaev, D. G.; Morokuma, K. *J. Am. Chem. Soc.* **2003**, *125*, 570–579.
- (14) Hildenbrand, K.; Schulte-Frohlinde, D. *Int. J. Radiat. Biol.* **1989**, *55*, 725–738.
- (15) (a) Bothe, E.; Schulte-Frohlinde, D. *Z. Naturforsch., C*. **1982**, *37*, 1191–1204. (b) Lemaire, D. G. E.; Bothe, E.; Schulte-Frohlinde, D. *Int. J. Radiat. Biol.* **1984**, *45*, 351–358. (c) Lemaire, D. G. E.; Bothe, E.; Schulte-Frohlinde, D. *Int. J. Radiat. Biol.* **1987**, *51*, 319–330.
- (16) Li, M.-J.; Liu, L.; Fu, Y.; Guo, Q.-X. *J. Phys. Chem. B* **2006**, *110*, 13582–13589.
- (17) (a) Becke, A. D. *J. Chem. Phys.* **1993**, *98*, 1372. (b) Stephens, P. J.; Devlin, F. J.; Frisch, M. J.; Chabalowski, C. F. *J. Phys. Chem.* **1994**, *98*, 11623.
- (18) Lee, C.; Yang, W.; Parr, R. G. *Phys. Rev. B* **1988**, *37*, 785.
- (19) Frisch, M. J.; et al. *Gaussian 03*, revision B.04; Gaussian, Inc.: Pittsburgh, PA, 2003.
- (20) (a) Malikin, V. G.; Malkina, O. L.; Eriksson, L. A.; Salahub, D. R. In *Modern Density Functional Theory, A Tool for Chemistry*; Seminario, J. M., Politzer, P., Eds.; Elsevier: New York, 1995. (b) Engels, B.; Eriksson, L. A.; Lunell, S. *Adv. Quantum Chem.* **1997**, *27*, 297.
- (21) (a) Hermosilla, L.; Calle, P.; García de La Vega, P. M.; Sieiro, C. *J. Phys. Chem. A* **2005**, *109*, 1114–1124. (b) Hermosilla, L.; Calle, P.; García de La Vega, P. M.; Sieiro, C. *J. Phys. Chem. A* **2006**, *110*, 113600–113608.
- (22) (a) Close, D. M. *Radiat. Res.* **1997**, *147*, 663–673. (b) Hole, E. O.; Nelson, W. H.; Sagstuen, E.; Close, D. M. *Radiat. Res.* **1992**, *130*, 148–159.
- (23) de Leeuw, H. P. M.; Haasnoot, C. A. G.; Altona, C. *Isr. J. Chem.* **1980**, *20*, 108.
- (24) Feigon, J.; Wang, A. H. J.; van der Marel, G. A.; van Boom, J. H.; Rich, A. *Nucleic Acids Res.* **1984**, *12*, 1243.
- (25) Tran-Dihn, S.; Taboury, J.; Neumann, J. M.; Huynh-Dinh, T.; Genissel, B.; Langlois d'Estaintot, B.; Igolen, J. *Biochemistry* **1984**, *23*, 1362.
- (26) Davis, P. W.; Hall, K.; Cruz, P.; Tinoco Jr., I.; Neilson, T. *Nucleic Acids Res.* **1986**, *14*, 1279.
- (27) Davis, P. W.; Adamiak, R. W.; Tinoco Jr., I. *Biopolymers* **1990**, *29*, 109.
- (28) Agback, P.; Sandström, A.; Yamakage, S. I.; Sund, C.; Glemarec, C.; Chattopadhyaya, J. *J. Biochem. Biophys. Methods* **1993**, *27*, 229.
- (29) Agback, P.; Glemarec, C.; Yin, L.; Sandström, A.; Plavec, J.; Sund, C.; Yamakage, S. I.; Viswanadham, G.; Rousse, B.; Puri, N.; Chattopadhyaya, J. *Tetrahedron Lett.* **1993**, *34*, 3929.
- (30) Röder, O.; Ludemann, H. D.; vonGoldammer, E. *Eur. J. Biochem.* **1975**, *53*, 517.
- (31) Plavec, J.; Thibaudeau, C.; Viswanadham, G.; Sund, C.; Chattopadhyaya, J. *J. Chem. Soc., Chem. Commun.* **1994**, 781.
- (32) Colson, A.-O.; Sevilla, M. D. *Int. J. Radiat. Biol.* **1995**, *67*, 627–645.
- (33) Yushchenko, D. A.; Shvadchak, V. V.; Klymchenko, A. S.; Duportail, G.; Pivovarenko, V. G.; Mély, Y. *J. Phys. Chem. A* **2007**, *111*, 10435–10438.